Photolysis of Compressed Sodium Azide (NaN_3) as a Synthetic Pathway to Nitrogen Materials

Suhithi M. Peiris*,† and Thomas P. Russell†

Chemistry Division, Naval Research Lab, Washington, D.C. 20375

Received: April 17, 2002; In Final Form: September 27, 2002

The potential syntheses of pure nitrogen materials may involve photolysis of azide compounds. In this work, compressed solid samples of NaN_3 were photolyzed in gem anvil cells at pressures up to 5.0 GPa. Reaction rates and mechanisms for the photolytic processes were studied using single-shot time-resolved (microsecond scale) absorption spectroscopy. Two broad absorption bands due to reaction intermediates were observed at 300 and 700 nm. Tentative assignments of the reaction intermediates and their reaction rates were used to help elucidate the potential for high-pressure syntheses of novel nitrogen structures. Finally, recovered products were analyzed with infrared and Raman vibrational spectroscopy.

Introduction

High-energy density materials that burn with release of environmentally clean byproducts are of interest as more efficient fuels/propellants that generate larger thrusts for supersonic and space applications. They also have potential applications as explosives and other energy storage systems. The most promising material would be an all-nitrogen compound in a structure with high lattice energy, which would also be a relatively inert solid at room temperature. Conceivably such a solid would decompose, producing only N_2, a relatively innocuous product (air being composed of 70% N_2).

Past efforts to synthesize all-N materials have established the azide radical ($N_3^{\bullet}$) as a useful starting material.[1−4] The earliest mention of an all-N component of a synthesized material in published literature, is in 1956 by Huisgen and Ugi.[5] On the basis of ^{15}N studies they postulated that a thermally unstable product resulting from a reaction of benzenediazonium chloride with lithium azide in methanol at −40 °C, was phenylpentazole. Subsequent work showed that electron donating substituents in the para position of the benzene ring stabilized the pentazole ring system.[6] A series of para-substituted derivatives were then isolated at low temperatures. The most stable of these substituted pentazoles, 4-(dimethylamino)phenylpentazole, decomposes only at 50 °C. A crystal structure for this all-N ring was reported much later.[7] The measured N−N bond distances in the pentazole ring are in the range 1.30−1.35 Å. These distances are intermediate between single N−N bonds (1.45 Å) and double N═N bonds (1.25 Å), and therefore, the pentazole ring, with its 6π electrons and nearly equivalent bond lengths, is considered aromatic.

Later, during spectroscopic studies of the photoionization of azides in solution, pure nitrogen molecules were postulated.[8] Optical absorption studies showed the formation of transient species in solution. A prominent absorption detected at 278 nm was identified as the $N_3^{\bullet}$ radical in its $2\pi_g$ ground state. Subsequently, a spectroscopic and theoretical study of $N_6^{\bullet-}$ was reported.[3] In this reference, a transient visible absorption band observed at 700 nm, was assigned to $N_6^{\bullet-}$.

More recently, the pure nitrogen ion (N_5^+) was produced by Christe and Wilson.[4] They report that the N_5^+ cation needs to be accompanied by large anions such as AsF_5^- or SbF_5^-. The N_5^+ geometry is stabilized by a resonance between two structures, each with four N−N bonds with bond orders of 1, 1.5, 2.5, and 3. The synthesis of N_5^+ also includes the reaction of N_2^+F with the azide anion N_3^-.[4]

The efforts reported here focus on the photolytic synthesis of N materials from solid azides at high pressure. Photolysis of azide ions occurring by one-photon absorption at 230 nm or two- and three-photon absorption (at blue and green wavelengths) are known to yield azide radicals.[8−10] Under highly confined conditions such as elevated pressure azide radicals may bond with other azide species or nitrogen species to form larger high-N molecules. This paper presents our results on NaN_3 and proposes a photolysis reaction mechanism for this relatively inert and widely used material.

Procedure

Samples were loaded in Merrill-Bassett type pressure cells containing either diamond or sapphire anvils with 350−800 μm wide culet flats.[11] One hundred micrometer thick 301 stainless steel gaskets drilled with 250−550 μm diameter holes were placed between the anvils. A ruby sphere about 10 μm in diameter was placed with the sample to measure the initial pressure applied.[12]

In our initial experiments we found that NaN_3 reacted with air to form an undesired Na_2CO_3 passivation layer. When working with micro quantities, upon reaction of NaN_3, the passivation layer was sufficiently significant to be observed by IR spectra. Consequently in later experiments, NaN_3 powders were stored, handled, and loaded into pressure cells in a dry N_2-purged glovebox. To ensure good light transmittance and optically thin NaN_3 samples, the azide was loaded between two layers of NaCl powder.

The experimental arrangement to measure time-resolved absorption is shown in Figure 1. Details of this experimental method can be found elsewhere.[13,14] A single pulse from a flashlamp-pumped dye laser (514 nm, 7−8 μs pulse duration,

* Corresponding author. E-mail address: PeirisSM@ih.navy.mil, Work Phone: (301) 744-4252.

† Now at: Research and Technology Department, Naval Surface Warfare Center - Indian Head Division, 101, Strauss Avenue, Indian Head, Maryland 20640.

10.1021/jp025963u
Published on Web 01/17/2003

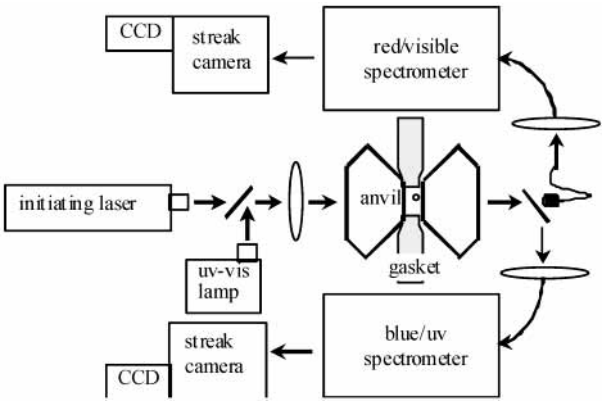

Figure 1. Experimental setup of the single-shot time-resolved spectroscopy system used to study reaction chemistry at high pressure. Both the laser pulse used to initiate photolysis and the 25 μs UV−vis source pulse used as incident absorbance were focused into the sample within the diamond cell.

3−50 J/cm^2 fluence) is used to photolyze the samples. Simultaneously, a source lamp for incident absorption provides light covering the wavelength region 250−900 nm. The pulse duration of this absorption source lamp is 25 μs. A dichroic beam splitter separates the light transmitted through the sample and anvils between two wavelength regions of 250−420 nm and 550−850 nm. The transmitted light in each wavelength region is further dispersed in wavelength by a spectrometer and is streaked in time normal to the wavelength axis by a Hamamatsu streak camera. CCD detectors then measure the intensities of the wavelength- and time-resolved light.

First, "prephotolysis" UV−vis transmission was recorded through the pressurized NaN_3 sample before initiating reaction with the laser. This transmission was considered a reference intensity $I_0(t,\lambda)$. The transmitted light during photolysis was similarly recorded to yield $I(t,\lambda)$. A "change in absorbance" (ΔA) was calculated with respect to the reference intensity.

$$\Delta A(t,\lambda) = \log(I_0/I)$$

Photodiodes monitored the light outputs of the initiating laser and the UV−vis source. These together with a digital signal analyzer were used to determine the start of the laser pulse assigned to be zero time ($t = 0$). Finally, a "postphotolysis" UV−vis transmission spectrum of the pressurized reaction remnants in the cell was recorded. The residue in the cell after photolysis was analyzed in situ at pressure with UV−vis, IR, and Raman spectroscopy. Subsequently, the cells were opened in a dry-nitrogen glovebag to unload the cell without exposing the sample to air. Once removed from the pressure cell, the samples were again analyzed (IR, Raman, UV−vis, and XPS) prior to and after exposure to air at ambient pressure.

Results

The "prephotolysis" absorption spectra of unreacted NaN_3 show an absorbance rising to 250 nm (This is the lower detection limit of our UV spectroscopy system). This absorption edge is assigned to the absorption of the N_3^- in the NaN_3 (230 nm). Once the NaN_3 photolysis is started with the laser pulse at time 0, changes in UV absorption (relative to prephotolysis absorption of NaN_3), show an increase in absorption intensity centered near 300 nm.

The right plot in Figure 2 represents a spectral sequence of this increase in absorption, showing time-resolved "change in absorbance" data dispersed by the UV spectrometer and measured at time intervals of 0.857 μs, obtained from a single-shot reaction at pressure. Notice the change in absorption gradually rising from about 360 nm to peak at about 300 nm. Previous photolysis studies of azides in solution showed that the $N_3^\bullet$ radical absorbs light at 277 nm.[9,10] The growth of the absorbance feature at 300 nm is postulated to be the formation of the $N_3^\bullet$ radical, since the azide in these experiments is in the solid state and at some pressure, when compared to the azide solutions used in the previous studies. Similarly, the second spectrometer dispersing visible wavelengths shows an absorption feature around 750 nm. Previous work by Workentine et al. reports the formation of $N_6^{\bullet-}$, which has a broad featureless absorption centered near 700 nm.[3] Hence, this second absorption feature in the visible is postulated to be $N_6^{\bullet-}$.

Figure 2 also shows how reaction profiles or kinetics are estimated from the change in absorbance data. Change in absorbance within a certain wavelength region around a particular wavelength is averaged and plotted against time. For these samples, 6 nm wavelength regions around the wavelengths of 300 and 700 nm were chosen. In Figure 2, the averaged region around 300 nm is marked by a rectangle in the plot on the left. On the right side of Figure 2 is a plot of the reaction profile calculated by averaging the change in absorbance within the area marked by a rectangle and plotted against time. This plot is considered a reaction profile.

Figure 3 shows reaction profiles of averaged change in absorbance versus time. This sample was at an initial pressure of 1.1 GPa (11 kbar). The UV absorbance (at 300 nm) shown as circles, increases to 5.2 μs, and then decreases, indicating the appearance and disappearance of $N_3^\bullet$ radicals. The visible absorbance (at 700 nm) shown as stars, achieves a maximum

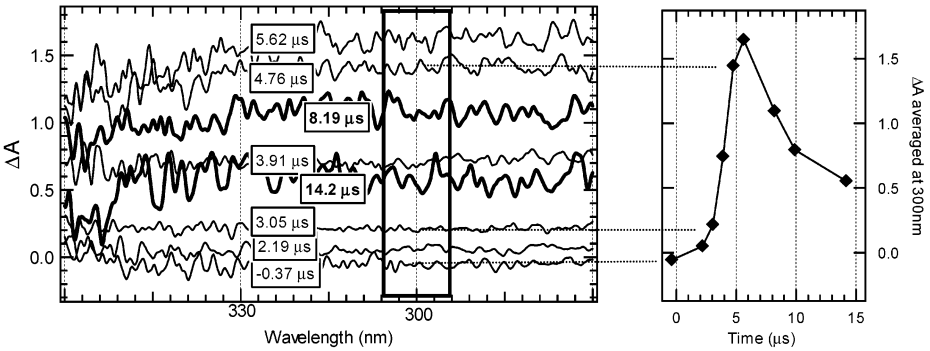

Figure 2. On the left is a plot of typical wavelength- and time-resolved changes in absorbance measured around 300 nm during the photolysis of NaN_3 at 1.1 GPa. The reaction profile is estimated by averaging the change in absorbance at each time over the wavelength region denoted by the rectangle. On the right is the reaction profile or change in absorbance averaged around 300 nm versus time. The dotted lines are included to show the averaged absorbance values on the left plot that yielded the data on the right plot.

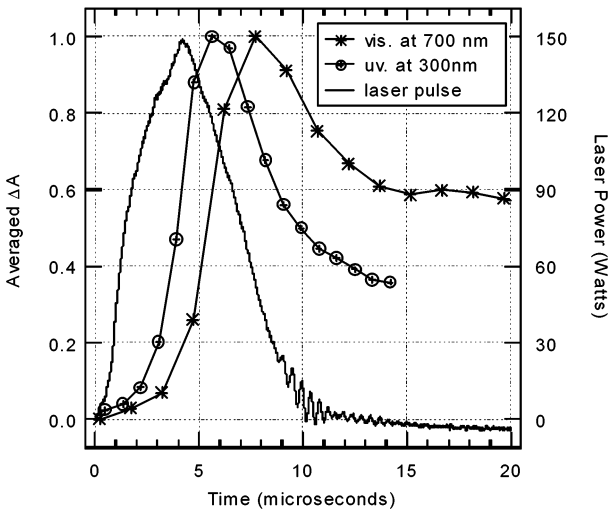

Figure 3. Change in absorbance averaged at 300 nm from the UV spectrometer, and the change in absorbance averaged at 700 nm from the vis spectrometer versus time, to show typical reaction profiles at 1.1 GPa. The solid lines are not the fitted curve. They are added to show the reaction profile. The laser pulse is included to show its time profile.

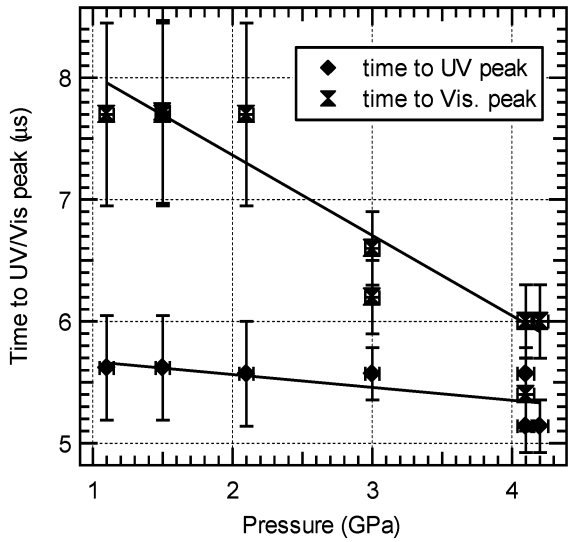

Figure 4. Time (from the start of the laser pulse) to maximum absorbance averaged at 300 nm and time (from the start of the laser pulse) to maximum absorbance averaged at 700 nm, plotted versus the initial pressure in the anvil cell. The magnitudes of the bracketed lines indicate uncertainties in the measurement of time and pressure. The solid lines are least-squares fits to the time-to-peak data from the two wavelength regions.

at 7.8 μs, indicating the formation of $N_6^{\bullet-}$. The solid line shows the laser pulse, which peaks after 4 μs and then falls off by 9 μs.

The pressure dependence of the postulated reaction intermediates $N_3^{\bullet}$ and $N_6^{\bullet-}$ was determined up to 4.0 GPa (40 kbar) and are shown in Figure 4. The error bars associated with the time measurements arise from the rate of the streak camera. The larger the time-axis error bars in Figure 4, the slower the streak camera was streaked. The errors associated with the pressure measurements are within the symbol used for data. A linear-least-squares fit of a straight line to the UV-peak data shows a very shallow slope that fits within the error of the time measurements, indicating that the time to UV peak does not depend on pressure, at least within the pressure range investigated here. Instead, UV absorbance always starts rising when the laser fluence pulse rises and falls off when the intensity of the laser pulse drops, indicating that the production of $N_3^{\bullet}$ radicals is primarily photolytic. However, as demonstrated in Figure 4, the $N_6^{\bullet-}$ temporal profile appears to depend on pressure. In this pressure range, the time to maximum absorbance of $N_6^{\bullet-}$ decreases from 8 to 6.0 μs, suggesting that higher initial pressures result in higher rates of formation of $N_6^{\bullet-}$.

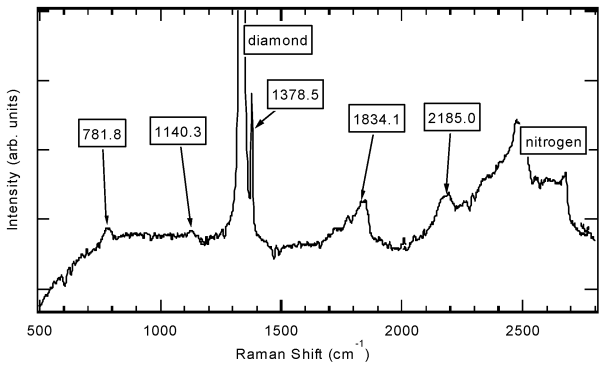

Figure 5. Micro-Raman spectrum of the red liquid residue compressed within the diamond cell. The Raman lines originating from the red liquid disappear when the cell pressure is reduced to ambient.

TABLE 1: Observed Raman Frequencies of the Red Liquid Residue and Calculated Frequencies of Other Possible Species

species	symmetry	raman modes (cm^{-1})	ref.
red liquid	?	781, 1140, 1378, 1894, 2185	our data
NaN_3	D_{3d}	122, 1267, 1358	16
N_7^-	C_{2v}	939, 1252, 1299, 2151	17
ClN_3	C_s (linear)	547, 721, 1231, 2191	15
Cl_2N_6	C_1 (boat)	835, 1145, 1954	15

The products remnant in the anvil cell upon completion of photolysis, were studied with optical light microscopy, IR, and Raman spectroscopy. In all samples, optical microscopy indicated a silver-colored solid. When exposed to air the silver solid reacted to form a liquid (as expected for $2Na + 2H_2O \rightarrow 2NaOH + H_2$), indicating that it is most likely Na metal. In all samples, Raman spectroscopy indicated N_2 formation. Optical microscopy of the cells in which enough azide had been photolyzed to enable clear observation of products, revealed a red liquid residue. No strong absorbance from this liquid was observed in the wavelength regions 270−420 and 550−850 nm. Micro-Raman spectroscopy of the red liquid yields five Raman-active vibrational modes at 782, 1140, 1378, 1834, and 2185 cm^{-1}. (See Figure 5 and Table 1.) Unfortunately, no new IR modes were observed, probably because of the very weak intensity of N−N stretches or the very small product quantities present. Once pressure is released, the red liquid vanishes, indicating that the red liquid is stable only at high pressure and either evaporates or decomposes to gaseous products upon release of pressure.

Discussion

During photolysis, a UV absorption peak is observed around 300 nm. Because $N_3^{\bullet}$ absorbs at 277 nm, this UV absorbance peak is interpreted as absorbance by azide radical being produced.[9,10] Because $N_3^{\bullet}$ production coincides with the laser pulse and is independent of pressure it is considered a photolytic process. The photolytic mechanism for $N_3^{\bullet}$ formation is as follows.

$$N_3^- + h\nu \rightarrow N_3^{\bullet} + e^-$$

$$Na^+ + e^- \rightarrow Na$$

Once the laser pulse ends, $N_3^\bullet$ radicals are no longer continuously produced and a decrease in the $N_3^\bullet$ concentration is observed. The concentration of $N_3^\bullet$ can decrease via any of three pathways.

$$N_3^\bullet + e^- \rightarrow N_3^- \quad \text{(a)}$$

$$N_3^\bullet \rightarrow N^\bullet + N_2 \quad \text{(b)}$$

$$N_3^\bullet + N_3^- \rightarrow N_6^{\bullet -} \quad \text{(c)}$$

Because metallic Na, N_2 and other products are observed, $N_3^\bullet$ most likely continues to react via pathways (b) or (c), instead of simply converting back to the anions by pathway (a).

Because a second intermediate with absorbance centered near 750 nm is observed during reaction, and this intermediate is proposed to be $N_6^{\bullet -}$, pathway (c) is proposed as the mechanistic path. In addition, enhanced confinement or higher pressure favors the reaction of $N_3^\bullet + N_3^-$ to produce $N_6^{\bullet -}$, as shown in Figure 4. Therefore, pathway (c) is more consistent with La Chatelier's principle than pathway (b), in that the production kinetics of a single species by the combination of two different species should (and does) increase at higher pressures. Figure 3 also shows that the product $N_6^{\bullet -}$ is a transient intermediate and further reacts to produce other species.

If $N_6^{\bullet -}$ is produced, then several plausible mechanisms involving the reaction of $N_6^{\bullet -}$ may be suggested to constitute the red liquid product detected.

$$N_3^\bullet + N_6^{\bullet -} \rightarrow N_2 + N_7^- \quad (1)$$

$$N_3^\bullet + NaCl \rightarrow NaN_3 + Cl^\bullet \quad \text{(2a)}$$

$$N_6^{\bullet -} + 2Cl^\bullet \rightarrow Cl_2N_6 + e^- \quad \text{(2b)}$$

One potential chainlike structure is N_7^-, while a potential ring structure could be Cl_2N_6.[15] N_7^- could be produced by the reaction of $N_3^\bullet$ and $N_6^{\bullet -}$, as shown in reaction 1. Cl_2N_6 is a feasible product as the pressure medium used is NaCl and the $N_3^\bullet$ produced could react with NaCl to release $Cl^\bullet$ radicals as in reaction 2a. Then the $N_6^{\bullet -}$ can be stabilized in the Cl_2N_6 ring structure via reaction with $Cl^\bullet$ radicals as in reaction 2b.

A wide range of N-materials was considered as possible structures of the red liquid residue. The most possible structures were selected by comparing the calculated Raman frequencies of these structures against the experimentally obtained Raman frequencies of the red liquid. (The calculations were performed using the Gaussian 98 and ACES II programs, employing either the Hartree−Fock self-consistent-field method or the density-functional theory (B3LYP) method, with basis sets of either 6-311G** or 6-31G**, and scaled with the recommended scaling factors.[15]) These frequencies are presented in Table 1. Considering Cl_2N_6, three of the observed frequencies (781, 1140, and 1894 cm^{-1}) could correspond to the calculated modes 835, 1145, and 1954 cm^{-1}. Then the two "azide like" modes of 2185 and 1378 cm^{-1} would be attributed to either liquidlike azide or azide ions distorted from its usual linear symmetry. Alternatively, all five of the observed Raman modes could belong to N_7^-, a W-shaped structure that includes "azide-like" linear branching.

Conclusions

The reaction mechanism and kinetics of the high-pressure photolysis of NaN_3 was investigated as a potentially novel method of synthesizing all-N materials. Time- and wavelength-resolved absorbance measurements indicated the formation of two intermediates. The first intermediate absorbing in the UV (300 nm), peaks about 5 μs after the laser pulse initiates reaction when the laser fluence is maximum, and is proposed to be $N_3^\bullet$ radicals. The second intermediate, absorbing around 750 nm, is tentatively identified as $N_6^{\bullet -}$. The kinetics of the production of this intermediate is enhanced by pressure. Therefore, the proposed reaction mechanism for the photolysis of NaN_3 is described by the equations below.

$$Na^+ + N_3^- \rightarrow Na + N_3^\bullet$$

$$N_3^\bullet + N_3^- \rightarrow N_6^{\bullet -}$$

The final products observed are metallic Na, N_2, and in certain samples, a red liquid residue stable only at pressure. The Raman modes of the red liquid suggest it is either N_7^- or Cl_2N_6 where $Cl^\bullet$ radicals are obtained from the pressure medium NaCl.

Acknowledgment. S.M.P. thanks Dr. G. Pangilinan for his assistance in the lab and for obtaining the Raman spectra.

References and Notes

(1) Vogler, A.; Wright, R. E.; Kunkley, H. *Angew. Chem., Int. Ed. Engl.* **1980**, *19*, 717.
(2) Gorini, J. A. C.; Farras, J.; Feliz, M.; Oliverella, S.; Sole, D.; Vilarrasa, J. *J. Chem. Soc., Chem. Commun.* **1986**, *1986*, 959.
(3) Workentine, M. S.; Wagner, B. D.; Negri, F.; Zgierski, M. Z.; Lusztyk, J.; Siebrand, W.; Wagner, D. M. *J. Phys. Chem.* **1995**, *99*, 94.
(4) Christe, K. O.; Wilson, W. W. *Angew. Chem., Int. Ed. Engl.* **1999**, *38*, 2004.
(5) Huisgen, R.; Ugi, I. *Angew. Chem.* **1956**, *68*, 706.
(6) Ugi, I.; Perlinger H.; Behringer, L. *Chem. Ber.* **1958**, *91*, 2324.
(7) Wallis, J. D.; Dunitz, J. D. *J. Chem. Soc., Chem. Commun.* **1983**, *1983*, 910.
(8) Hayon, E.; Simic, M. *J. Am. Chem. Soc.* **1970**, *92*, 7486.
(9) Burak, D.; Shapira, D.; Treinin, J. *Phys. Chem.* **1970**, *74*, 568.
(10) Butler, J.; Land, E. J. *Radiat. Phys. Chem.* **1984**, *23*, 265.
(11) Russell, T. P.; Piermarini, G. J. *Rev. Sci. Instrum.* **1997**, *68*, 1835.
(12) Piermarini, G. J.; Block, S.; Barnett J. D.; Forman R. S. *J. Appl. Phys.* **1975**, *46*, 2774.
(13) Russell, T. P.; Allen, T. M.; Gupta, Y. M. *J. de Physique IV* **1995**, *5*, 553.
(14) Russell, T. P.; Allen, T. M.; Gupta, Y. M. *Chem. Phys. Lett.* **1997**, *267*, 351.
(15) Mowery, R. C. Private communication, 1999.
(16) Bryant, J. I. *J. Chem. Phys.* **1964**, *40*, 3195.
(17) Michels, H. H.; Montgomery, J. A.; Christe, K. O.; Dixon, D. A. *J. Phys. Chem.* **1995**, *99*, 187.